International Journal of Electrical and Computer Engineering (IJECE)
Vol. 8, No. 5, October 2018, pp. 2967~2978
ISSN: 2088-8708, DOI: 10.11591/ijece.v8i5.pp2967-2978

Adaptive Multi-state Millimeter Wave Cell Selection Scheme for 5G communications

Mothana L. Attiah[1], Azmi Awang Md Isa[2], Zahriladha Zakaria[3], Nor Fadzilah Abdullah[4], Mahamod Ismail[5], Rosdiadee Nordin[6]

[1,2,3]Centre for Telecommunication Research and Innovation (CeTRI), Faculty of Electronic and Computer Engineering (FKEKK), Universiti Teknikal Malaysia Melaka (UTeM), Malaysia
[1]Department of Computer Engineering, Electrical Engineering Technical College, Middle Technical University, Iraq
[4,5,6]Faculty of Engineering and Built Environment, Universiti Kebangsaan Malaysia (UKM), Malaysia

Article Info

Article history:

Received Dec 17, 2017
Revised Apr 13, 2018
Accepted Jul 25, 2018

Keyword:

5G communications
Hybrid mmWave (BS) aproach
Mmwave frequency bands
Multiple mmwave connections
Outage probability

ABSTRACT

Millimeter wave bands have been introduced as one of the most promising solutions to alleviate the spectrum secrecy in the upcoming future cellular technology (5G) due the enormous amount of raw bandwidth available in these bands. However, the inherent propagation characteristics of mmWave frequencies could impose new challenges i.e. higher path loss, atmospheric absorption, and rain attenuation which in turn increase the outage probability and hence, degrading the overall system performance. Therefore, in this paper, a novel flexible scheme is proposed namely Adaptive Multi-State MmWave Cell Selection (AMSMC-S) through adopting three classes of mmWave base stations, able to operate at various mmWave carrier frequencies (73, 38 and 28 GHz). Two mmWave cellular Grid-Based cell deployment scenarios have been implemented with two inter-site-distances 200 m and 300 m, corresponding to target area of (2.1 km2) and (2.2 km2). The maximum SINR value at the user equipment (UE) is taken in to consideration to enrich the mobile user experience. Numerical results show an improvement of overall system performance, where the outage probability reduced significantly to zero while maintaining an acceptable performance of the 5G systems with approximately more than 50% of the mobile stations with more than 1Gbps data rate.

Corresponding Author:

Mothana L. Attiah,
Department of Telecommunication Engineering,
Faculty of Electronic and Computer Engineering,
Universiti Teknikal Malaysia Melaka,
Hang Tuah Jaya, 76100 Durian Tunggal, Melaka, Malaysia.
Email: mothana.utem@gmail.com

1. INTRODUCTION

Over the last decade, global telecom companies along with the forecasting groups were talking about global data traffic growth around the world in the range of (Exabyte). Nowadays, the talk about Zettabyte has become remarkably broad. Wherein, in [1], [2] the annual global IP traffic will reach 3.3 ZB by 2021, up from 1.2 ZB per year (one billion Gigabytes) per month. Further, this extraordinary growth can be attributed to various advances in the technology with different factors form, more intelligence and multi-objective capabilities [3], [4]. These considerations had become a burden on the network and cloud operators pushing them to harness more efforts to satisfy the needs for extra bandwidth. Accordingly, millimeter wave frequencies (28 GHz, 38 GHz, and 70-80 GHz) have been proposed as a promising candidates to satisfy the future cellular communication (5G) requirements owning to the massive amount of spectrum bandwidth with an extremely high frequency ringing from 30–300 GHz [5]. Despite of the attractive opportunity offered by

mmWave frequency bands, there are unfavorable characteristics i.e. (i) the extra 20-40 dB path loss [6], [7];(ii) the tiny wavelength signals of mmWave frequencies (1 to 100 mm) often has been thought to contribute to higher attenuation through the air compared to the traditional below 6 GHz cellular band due to oxygen absorption and precipitation[8]; (iii) the high susceptibility to be blocked completely by many types of obstacle [9]-[12];(iv) the short coverage range of the mmWave with in (200 m) [13], [14].

On other hand, enhancing the spectral efficiency is another factor can effectively fuel the future demands taking advantages from several approaches [15]. Consequently, many approaches have been suggested in order to guarantee efficient and flexible resource utilization and hence, overcome the capacity of radio networks limitations. For instance, an integration of macro and small cells called dual connectivity (DC) was firstly introduced in Release (12) of LTE-A report [16], [17],built upon the functionality of the concept which so-called carrier aggregation (CA)[18]. In light of the above approach, *Multi-connectivity* (MC) architecture is presented in [19], [20] which is in one way or another inspired by the notion behind the concept of *dual connectivity*. Furthermore, an optimal cell placement technique have been used with the cooperation between microcells (MSs) and small cells (SCs) [21] to overcome the randomization of the mmWave cell placement.

Particularly, mmWave base stations need to be densely distributed throughout a small area in order to improve the coverage range and enhance the overall system performance [22]. However, the high-gain and the highly directional antenna arrays at the transmitter (TX) and the receiver (RX) reinforces the suitability of mmWave wireless communications [23]. As a result, in addition to the aforementioned studies there is a specific research activities embarked on a study of the characteristics of the millimeter wave as well as its enabling technologies, in which can be classified into two categories, mmWave measurement campaigns activities and mmWave communication QoS assessment. In terms of the first category introducing mmWave bands as promising candidates for 5G cellular system gives high priority for understanding of the special–behavior of these bands. Based on this, extensive studies and set of measurements are conducted in [24]-[33]. Although, a few measurement campaigns conducted at high frequency (above 6GHz), there are some system level assessments that obtained from those measurement campaigns, which opens up the road for building an initial perception of 5G communication's structure, MAC-Layer, system configurations, and its enabling technologies. Accordingly, the first QoS evaluation with respect to SINR and average rate of mmWave picocellular networks in a dense urban environment at 28GHz has been conducted in [34]. While, in [35] the same inter-site- distance in previous work (200m) has been taken to evaluate two mmWave frequencies (73 and 28 GHz). However, both of the aforementioned studies are performed and evaluated based on the initial propagation measurements in most challenging environment in New York City (NYC).

Capturing and analyzing the key distinguishing marks of mmWave cellular networks have been made using a tractable model developed in [36], and its extension in [37], which demonstrates that bandwidth would have minimal effect on the rate of noise-limited cell edge users (poor SINR user). In [38] the impact of self-body blocking phenomena in millimeter wave communication has been evaluated in which proves that even with self-body blocking mmWave outperforms the conventional cellular average rate. In [12], [39] were proposed a stochastic geometry frameworks for analyzing the coverage and rate in mmWave cellular networks to ensure the successful realization of utilizing high frequencies. In a more recent works, carrier frequencies above 6-GHz have been targeted as in [11], [40] with a novel methods have been targeted to characterize the benefits introduced by dynamic multi-connectivity techniques via exploiting coexistence between 4G and mmWave base stations toward the realization of 5G networks. Moreover, mmWave/sub-6 GHz Multi-Connectivity with relaying is considered in [41] for enriching user-centric with high end-to-end throughput in a cost-effective network deployment. Finally, in order to harvest the maximum benefit from emerging mmWave technologies an efficient spectrum access scheme has been proposed in [7], wherein, two hybrid spectrum accesses are utilized firstly, mmWave band with exclusive access and the second is pooled between multiple operators.

In this article, we extend our work in [42], through an extensive investigation and we present a useful assessment at extremely high carrier frequencies. However, different path loss model (the commonly used close-in reference distance model) has been considered in order to investigate other parameters which may affect the overall performance system as will be discussed in more detail later. New conceptual multiple connection framework for the future 5G cellular communication has been provided. It is fully introduced and analyzed consisting of a novel link-adaptive scheme (AMSMC-S), where UEs are capable of having parallel links to three base stations. However, UE can only choose one of them based on the quality of these links. According to the link-adaptive scheme, each user equipment attempts to rise up its own achievable data rate and reduce the disconnection-mode via a suitably selecting its mmWave cell which is often carry the highest signal-to-interference plus noise ratio (SINR). Three classes of mmWave cells/base stations (mBSs) are considered based on grid-based network deployment adopting three-millimeter wave frequencies (73, 38 and 28 GHz) for outdoor users and outdoor infrastructure. Furthermore, with the use of this scheme it can be

easily tested the impact of the adaptive/dynamic procedure under different parameters and different power constraints targeting more challenging environments to harvest and realize the benefit of the hybrid mmWave deployment.

The limitation of the dynamics of millimeter wave links and the large variations in signal level have been overcome in this work through utilizing efficient millimeter wave cell and user tracking mechanism inspired by the work in [40]. Our proposed scheme aims to guarantee both quality of service (QoS) and quality of experience (QoE) as well exploiting the available resiliency of (AMSMC-S) to overcome the quality of link degradation. Meanwhile, maintaining the co-channel interference in acceptable level and guaranteeing sufficiently high availability.

2. AMSMC-S SCHEME

Our proposed scheme derives from the combination of several concepts that focus on the most effected parameters such as average data rate and outage probability in addition to the densification of millimeter wave base stations deployment. Based on this, utilizing of our proposed scheme relies on providing a feasible optimal cell selection mechanism adopting different classes of millimeter wave cells. Each class of mmWave cells adopts different level of mmWave frequency bands. More preciously, our proposed scheme totally depends on maximum SINR value that delivered generally by either mmWave Master-Cell (mMC) or mmWave Slave-Cell (mSC). Further, the theoretical concept of our proposed scheme can be implemented through two main mechanisms as shown in Figure .3a and Figure .3b.

As depicted in Figure 3a and Figure 3b any mmWave cell offers grater SINR value to a certain terminal i.e. (mobile station, IoE, etc.) than others will be the serving cell to that terminal. For instance, based on AMSMC-S Mechanism with mMC D-M, the UE need to establish connection with another user or just surfing the net it will send request to both the neighboring mmWave Master-Cell/4G Cell and the mmWave Slave-Cell (mSC) then the mmWave Master-Cell/4G Cell will gather the channel quality of the three mmWave Slave-Cells (28GHz mBSs, 38GHz mBSs and 73GHz mBSs) in addition to the channel quality of itself. The higher mmWave cell channel quality the optimal selected serving cell for that terminal.

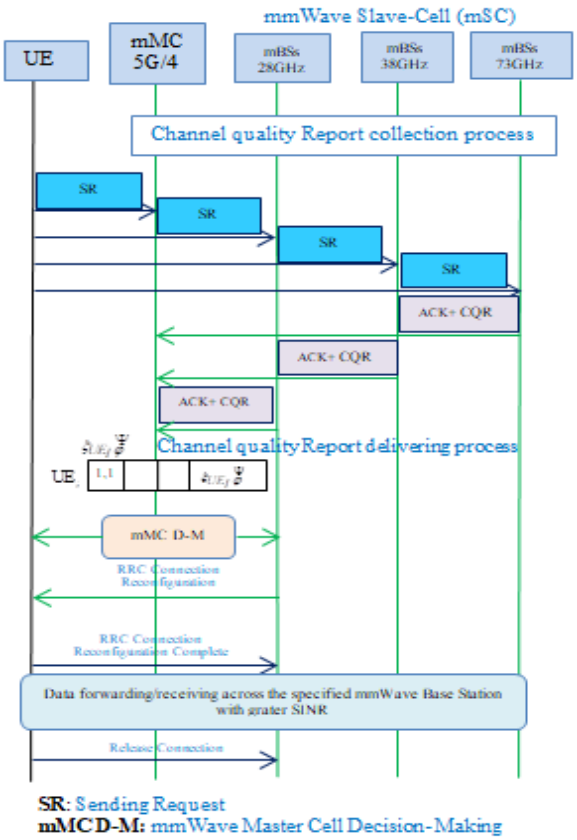

Figure 3. (a) AMSMC-S Mechanism with mMC D-M

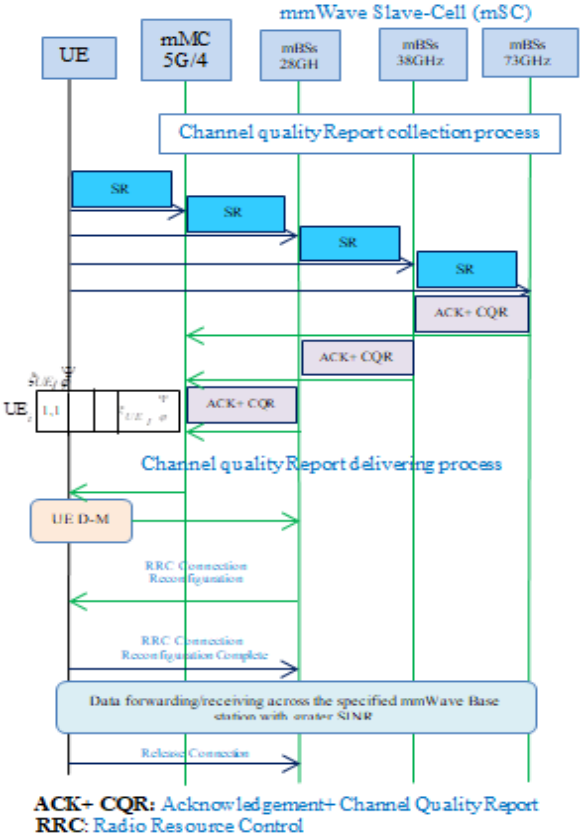

Figure 3. (b) AMSMC-S Mechanism with UE D-M

In Figure 3a and Figure 3b the 28GHs mBSs has greater SINR and therefore, it was chosen as optimal mmWave serving cell. Meanwhile, in the AMSMC-S Mechanism with UE D-M the UE need to establish connection with certain another UE will send request to both the neighboring mmWave Master-Cell/4G Cell (mMC) and the mmWave Slave-Cell (mSC) then receive back the AKC plus the channel quality reports for all neighboring mmWave Master-Cell/4G Cell and the mmWave Slave-Cell (mSC) for final decision-making choosing also the grater SINR mmWave Base station of both mMC and mSC same as the mMC D-M mechanism. The motivation of the selection of either AMSMC-S Mechanism with mMC D-M or AMSMC-S Mechanism with UE D-M is to guarantee flexible and optimal selection of the serving base station with lower both complexity and signal overhead. On other hand, the utilization of 4G as a master cell can provide good quality channel for pilots, control messages and other signaling might be necessary for the future cellular architecture needs.

3. RESEARCH METHOD

This section describes the network and simulator models and details the implementation aspects for all models are utilized in our proposed scheme (AMSMC-S) along with the reference scenarios. Moreover, the models are presented in full, detailing all functionality aspects related to the outage probability as well as the average rate and how one should apply them. Then a very detailed description of how the simulator was developed is performed. Four main distinct components are considered in our analytical framework as illustrated below:

3.1. Network Topology Deployment

Grid-based network topology with dense mmWave's cells deployment is adopted. The mmWave cells are assumed stationary during the entire simulation and observation period. However, it is possible to relay on semi-moving or semi-static millimeter wave cells in one case if those cells remain stationary without any change in the Line-of-Site (LOS) and Non-Line-of-Site (NLOS) environment in relation to the position of the users during the service delivery period for those UEs. More specifically, three classes of millimeter wave cells are chosen according to three mmWave frequencies (73, 38 and 28 GHz).

The chosen simulation's scenarios are implemented with two inter-site-distances (ISDs) 200 m and 300 m. Furthermore, two groups of 5G scenarios have been selected to investigate how viable adopting our proposed scheme (AMSMC-S). The first groups are 5G reference Stand-Alone mmWave networks deployment for the three mmWave cells operate at (73, 38 and 28 GHz) with the two inter-site-distances (ISDs). Figure 2a gives as an example of 5G Stand-Alone mmWave networks deployment for the cell range 150 m. The second groups are with hybrid mmWave network deployment combining all the above-mentioned frequencies with the same aspects in the reference scenario as shown in Figure 2b.

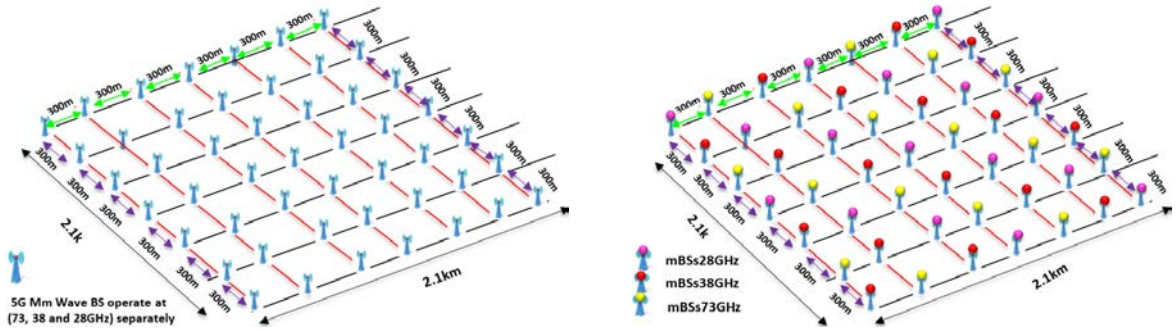

(a) (b)

Figure 2. (a) Millimeter wave Network Topology Deployments with Cell Range 150m
(b) Hybrid mmWave Network Topology Deployments with Cell Range 150m

3.2. Random UEs Generator

In the reference and our proposed scheme scenarios, users are assumed to be static and randomly distributed throughout the simulation area 2.2km × 2.2 km and 2.1km × 2.1 km for the two cell ranges (100-150 m) respectively. The UEs are positioned within a limited simulation length around the distributed

millimeter wave cells. As the separation distance between the mmWave base station and the users play a dominant role in determining the average receive signal, the UEs that are located closer to the millimeter wave cells will certainly receive high average signal and thus, achieving in most of the time high quality of service (QoS). Moreover, the power receiving value has directly impact on several parameters such as Signal-to-Interference Plus Noise Ratio (SINR) means that any improvement in the quality of the receive signal, in turn, improving the (SINR) value and hence, improving the overall system performance.

3.3. Mathematical models

In this paper, there are several key mathematical models are utilized. Some of them related to basic mobile communications and the rest to mmWave communication system which are designated and developed to be executed for producing one snapshot or more to get reasonable insights about the special behavior of the millimeter wave system. In order to calculate the received signal at the receiving antenna we consider the commonly used close-in reference distance path loss model represented in Equation (1) as in [14], [28], [31],[32] based on the propagation measurement campaigns conducted by NYU WIRELESS researchers for the three mmWave frequencies (73, 38 and 28 GHz).

$$PL(d_{\mathrm{UE}_i,\varphi}) = PL_{fs}(d_o) + 10 \times n \times \log_{10}\left(\frac{d_{\mathrm{UE}_i,\varphi}}{d_o}\right) + X_\sigma \ , \tag{1}$$

where $PL(d_{\mathrm{UE}_i,\varphi})$ stand for the average path loss in dB for a specific user or terminal UE_i and mmWave base station φ separation distance of $d_{\mathrm{UE}_i,\varphi}$ in meters, d_o is the close-in free space reference distance (1m), $PL_{fs}(d_o)$ stand for the close-in reference free space path loss in dB as identified in Equation (2), n stand for the average path loss exponent, X_σ stand for to zero mean Gaussian random variable with σ a standard deviation in (dB) since 10dB shadowing margin used in our work.

$$PL_{fs}(d_O) = 20 \times \log_{10}\left(\frac{4 \times \pi \times d_O}{\lambda}\right), \tag{2}$$

where λ denotes to the wavelength of the carrier frequency. The parameter of this model n and λ for the mmWave frequencies (73, 38 and 28 GHz) are listed in Table 1.

Table 1. Statistical Path-loss Parameter [14] ,[32], [43].

Variable	n [dB]	λ [mm]
28GHz	3.4	10.71
38GHz	2.6	7.78
73GHz	3.3	4.106

Generically, the average received signal power at the UEs calculated using the path loss model that is described earlier in [14], [28], [31], [32], combined with the link budget represented in the Equation (3) with log-scale as [35], [44]:

$$P_{r[dBm]} = P_{t[dBm]} + G_{t[dBi]} + G_{r[dBi]} - PL_{[\mathrm{dB}]}, \tag{3}$$

where P_r and P_t are the received and transmitted power of mmWave mBS respectively. G_t and G_r are the linear gains of the transmitter and the receiver antennas in dBi, respectively, PL stand for the average path loss in dB. Based on our proposed scheme we can rewrite the Equation (3) to fit the assumptions of the utilization of different classes of mmWave base station (mBSs) as shown below:

$$\mathrm{Pr}_{UE_i\ \varphi}^{\Psi}[dBm] = Pt_{\varphi}^{\Psi}[dBm] + Gt_{\varphi}^{\Psi}[dBi] + Gr_{\varphi}^{\Psi}[dBi] - PL_{UE_i\ \varphi}^{\Psi}[dB], \tag{4}$$

where Pt_{φ}^{Ψ} and $\mathrm{Pr}_{UE_i\ \varphi}^{\Psi}$ are the received and transmitted power of mmWave mBS respectively, with specific frequency band Ψ and with a certain number of φ ,since φ depends on the number of mBSs that deployed throughout the simulation area, G_t and G_r are the linear gains of the transmitter and the receiver antennas in

dBi, respectively, *PL* stand for the average path loss in dB. Ψ is considered as a set of sub-channel offered by a three classes of mmWave base stations, $\Psi \in S$ since S =[1, 2, 3] and each value of S represent a certain value of sub-channel of the three (73, 38 and 28 GHz) respectively.

$$\Psi = \begin{cases} \text{if } S=1 \text{ represents 73GHz mmWave Base Station} & \varphi = 1,2,3.....\varphi_n \\ \text{if } S=2 \text{ represents 38GHz mmWave Base Station} & \varphi_n \text{ depends on the number of mBSs} \\ \text{if } S=3 \text{ represents 28GHz mmWave Base Station} & \end{cases}$$

Basically, to measure system interference and examine its impact on network functionality, the SINR of a specific user/terminal expressed by UE_i connected to mBS Ψ under the determined number of φ is calculated based on the Equation (5) [45]:

$$\xi_{UE_i\varphi}^{\Psi} = \frac{\Pr_{UE_i\varphi}^{\Psi}}{\sum_{\varphi=1}^{N} I_{UE_i}^{\Psi} + \eta^{\Psi}}, \quad (5)$$

where $\xi_{UE_i\varphi}^{\Psi}$ is the Signal-to-interference plus noise ratio; $I_{UE_i\varphi}^{\Psi}$ is the interference received by the receiver UE_i from the only same class of neighboring mBS Ψ except the serving mBS φ; η^{Ψ} is the additive white noise power at the connected receiver UE_i connected to mBS with specific value of Ψ. The additive white noise power $\eta_{UE_i}^{\Psi}$ at the connected receiver UE_i with mmWave base station Ψ given by the Equation (6)[44]:

$$\eta_{UE_i}^{\Psi} = 10\times\log 10\left(KT_{sys}\right) + 10\times\log 10\left(W_{UE_i}^{\Psi}\right) + NF_{UE_i}^{\Psi}, \quad (6)$$

where $10\times\log 10\left(KT_{sys}\right)$ is equal to -174 dBm/Hz for a system temperature of $17C^{\circ}$; $NF_{UE_i}^{\Psi}$ is the Noise Figure of the receiver connected to Ψ in dB, set to 6dB. The calculated values of the Signal-to-interference plus noise ratio ($\xi_{UE_i\varphi}^{\Psi}$) are made to provide further user channel capacity calculation, thus the average rate of overall mmWave system can be calculated using Shannon capacity theory is shown in Equation (7) [45]:

$$C_{UE_i\varphi}^{\Psi} = M\times\left(\frac{W_{UE_i}^{\Psi}}{n}\right)\times\log_2\left(1+\xi_{UE_i\varphi}^{\Psi}\right), \quad (7)$$

where M denotes to the number of antenna arrays in the connected mmWave base station; $W_{UE_i}^{\Psi}$ denotes to the total amount of bandwidth of the specified Ψ. $\xi_{UE_i\varphi}^{\Psi}$ denotes to the Signal-to-interference plus noise ratio of the UE_i channel, n denotes to the number of users/terminals.

4. RESULTS AND DISCUSSION

Once the cornerstone of the 5G scenarios adopting millimeter wave technology with and without our proposed scheme (AMSMC-S) have been presented with more details about its consideration and overview structure, the next step is to evaluate the overall 5G mmWave system performance according to the aforementioned scenarios. This section tries to answer a few research questions as stated:

a. How does a flexible wireless system provided by our proposed scheme can reduce the outage probability and maximize the overall system average rate?
b. How viable our (AMSMC-S) scheme to reduce the complexity of the 5G system deployment?

The answers of two aforementioned questions with the evaluation of the two performance metrics along with simulation parameter settings as in Table 2 will be the focus of attention in the following subsections.

Table 2. Simulation Parameter Settings

Parameters	Settings
mmWave Base Station Layout	Grid-based Cell Deployment
mmWave Base Station density	49-Cell and 121-Cell
UE layout	Uniform random distribution
UE density	245 users/km2
Area of simulation	2.2 km^2 and 2.1 km^2
Inter-site distance (ISD)	200m and 300m
mBS Carrier frequency	73, 38 and 28 GHz
mBS Transmit power	30 and 20 dBm (downlink)
Noise Figure (BS)	5dB
Variant of white Gaussian noise	-174 dBm/Hz
Noise Figure (MS)	7dB
mBS antenna	8 × 8 uniform linear array
mBS Bandwidth	(2.5, 1.5 and 1 GHz) for (73, 38 and 28 GHz) respectively
Overhead Percentage	20% of the total amount of bandwidth

4.1. SINR Empirical Probability

A proper interference analysis can be achieved once we have a realistic conclusion about the impact of dense mmWave cells deployment in an urban scenario. Therefore, it is essential to study the signal-to-interference plus noise ratio (SINR) and its impact on 5G system since it represents a key system interference indicator. In this context, Figures 4,5,6, and 7 show the empirical cumulative distribution functions (CDF) of the downlink SINR distribution for the three mmWave frequencies (73, 38 and 28 GHz) which are deployed separately throughout the simulation area 2.1 km^2 and 2.2 km^2 with the cell ranges (150m-100m) respectively.

Two different TX power constraints (30 and 20 dBm) are considered along with the empirical (CDF) of downlink SINR distribution of the mmWave system adopting our proposed (AMSMC-S) scheme. The black color curve represents the empirical (CDF) of SINR of a mmWave communication system with (AMSMC-S) scheme. While, the rest represent the SINR distribution of the three mmWave frequencies (73, 38 and 28 GHz) which are deployed separately (stand-alone network deployment).

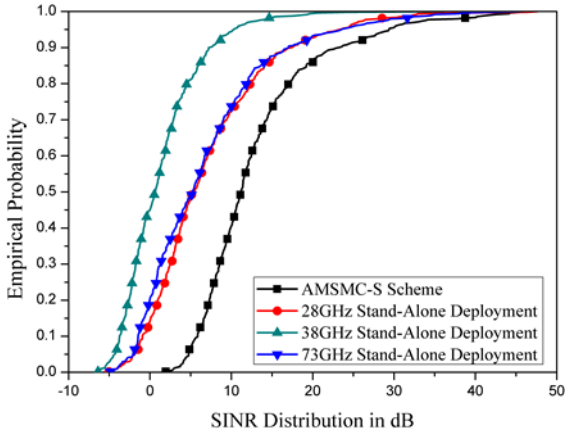

Figure 4. Downlink SINR CDF-Plot at (73, 38 and 28 GHz) for stand-alone deployment and our proposed (AMSMC-S) Scheme with Pt= 30 dBm (150 m cell range)

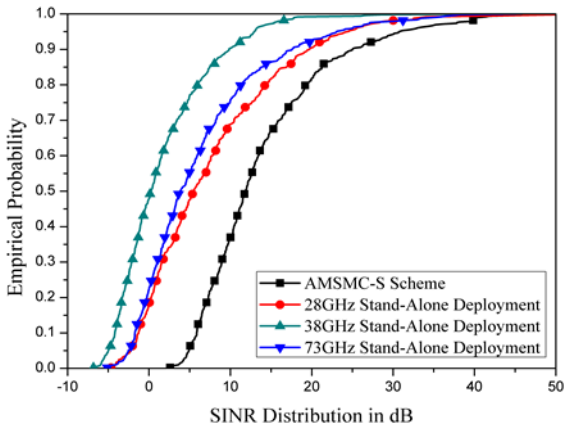

Figure 5. Downlink SINR CDF-Plot at (73, 38 and 28 GHz) for stand-alone deployment and our proposed (AMSMC-S) Scheme with Pt= 20 dBm (150 m cell range)

As can be observed from the SINR distribution depicted in Figure 4, 5, 6, and 7 our proposed scheme achieves sophisticated improvement in reducing the outage probability percentage of the mmWave frequencies to zero providing new conceptual mmWave deployment to be adopted soon in the future cellular communication (5G). Hence, the outage problem that resulted from the dynamic fluctuation of the link of mmWave frequencies due its characteristics has significantly overcome. In addition, after extensive iteration of the simulation, we carried out that any increasing in the TX power value gains relatively lowers outage probability with respect to the UE's location in terms of the three classes of the mmWave (mBSs). Moreover, even with the cell range of 150m, low outage probability can be achieved if the UE's are closer to the millimeter wave base stations. Overall, for the comparison purpose between our proposed scheme

(AMSMC-S) and the state of the art regarding to the coverage probability (outage probability) which is considered as the first performance metric.

The outage probability percentages that have been carried out adopting our proposed scheme reduced significantly which enable the cell-edge users to have SINR more than (2dB) as compared to the outage probability percentages that have been carried out in [7], [13], [34], [35], wherein, the cell-edge users experience SINR lower than zero. additionally, the mmWave base station density in our work less than that ones in the aforementioned benchmark studies. In order to sum-up the coverage probability evaluations taking into account the simulation area (2.1 km2 and 2.2 km2) with the two allocated power transmission constraints (30dBm-20dBm), the outage probability percentages of the aforementioned scenarios (5G) have been gathered to build a clear vision of our proposed scheme as compared to the 5G mmWave stand-alone reference scenarios as shown in Figure 8 and Figure 9.

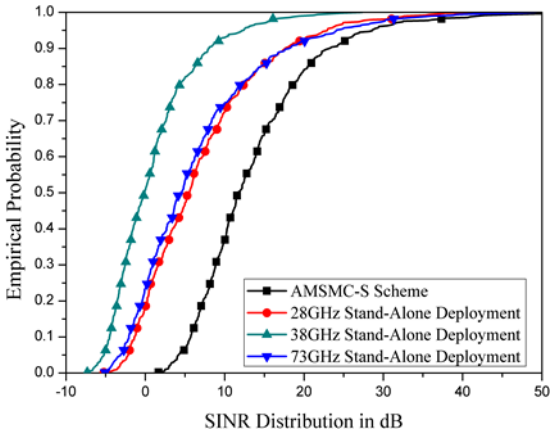

Figure 6. Downlink SINR CDF-Plot at (73, 38 and 28 GHz) for stand-alone deployment and our proposed (AMSMC-S) Scheme with Pt= 30 dBm (100 m cell range)

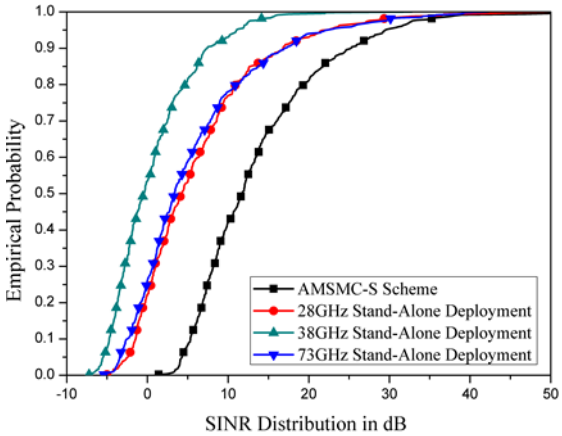

Figure 7. Downlink SINR CDF-Plot at (73, 38 and 28 GHz) for stand-alone deployment and our proposed (AMSMC-S) Scheme with Pt= 20 dBm (100 m cell range)

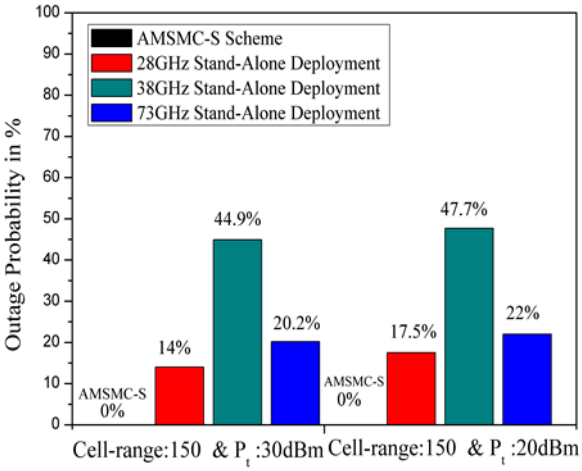

Figure 8. Overall Outage Probability Percentage of (73, 38 and 28 GHz) for stand-alone deployment and our proposed (AMSMC-S) Scheme with Pt=30dBm and 20dBm and cell range (150m)

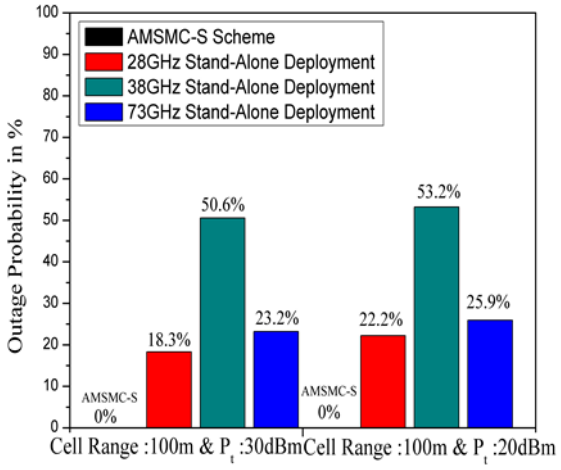

Figure 9. Overall Outage Probability Percentage of (73, 38 and 28 GHz) for stand-alone deployment and our proposed (AMSMC-S) Scheme with Pt=30dBm and 20dBm and cell range (100m)

4.2. Average Rate Distribution

By using Shannon's law illustrated in the Equation (6) the average rate of (490) users that are randomly distributed adopting our scheme is more than (1Gbps) keeping in mind that the bandwidth splits

among all the users associated to the mBSs. Based in this encourage result, adopting 5G networks with hybrid mmWave bands will enable the successful life-changing services enriching the users with a truly immersive applications and feeding the needs for more advances technologies. Meanwhile, adopting mmWave frequencies with a massive MIMO technology will pay attention for 5G communications to be a promising technology to reverse the widening revenue gap and make it worthwhile for operators and service providers to invest again in innovative new services, and continue to propel increased productivity and efficiency. Figures 10,11,12, and 13 show the empirical (CDF) of the downlink average rate for our proposed scheme based on the cell range 150 m and 100m respectively with two TX power constraints (30 and 20 dBm) along with the empirical (CDF) of the downlink average rate of three mmWave frequencies of the reference (stand-alone deployment) scenarios.

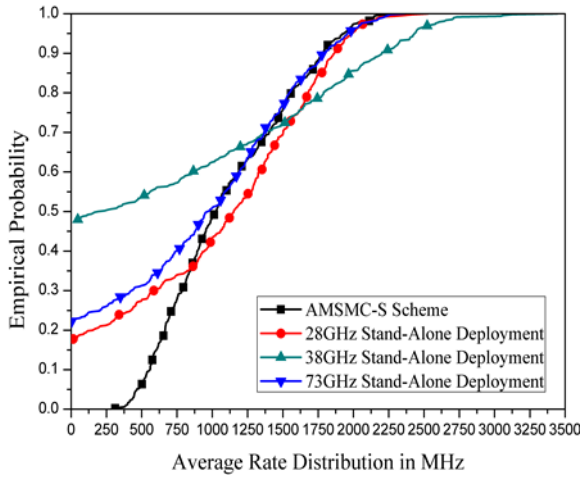

Figure 10. Downlink Average Rate CDF-Plot at (73, 38 and 28 GHz) for stand-alone deployment and our proposed (AMSMC-S) Scheme with Pt= 30dBm (150m cell range)

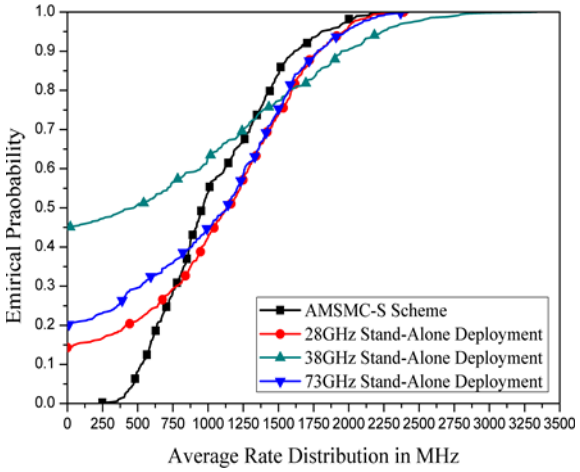

Figure 11. Downlink Average Rate CDF-Plot at (73, 38 and 28 GHz) for stand-alone deployment and our proposed (AMSMC-S) Scheme with Pt= 20dBm (150m cell range)

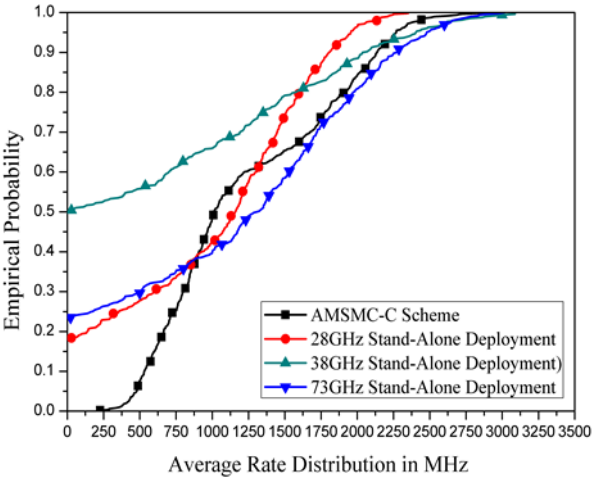

Figure 12. Average Rate Distribution (CDF-Plot) at (28, 38 and 73 GHz) with respect to stand-alone deployment and our proposed (AMSMC-S) Scheme with Pt= 30dBm (100 m cell range)

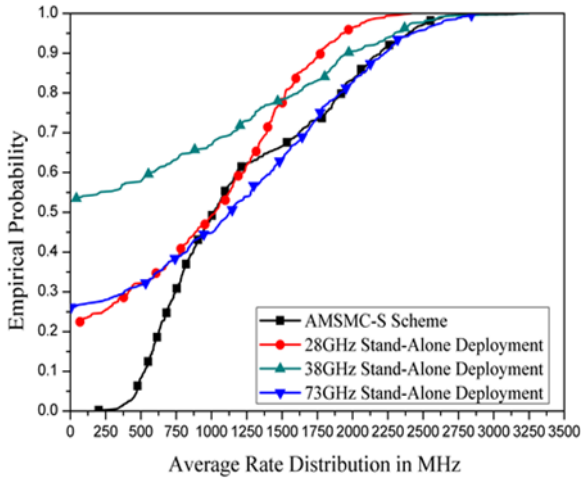

Figure 13. Downlink Average Rate CDF-Plot at (73, 38 and 28 GHz) for stand-alone deployment and our proposed (AMSMC-S) Scheme with Pt= 20dBm (100 m cell range)

Through the empirical (CDF) plot of the downlink average rate per user of the reference (stand-alone deployment) scenario that are illustrated in the graphs above, what can be deduced that even with the enormous amount of the indispensable spectrum bandwidth available in mmWave frequencies,

severe limitation in the data rate is existed due the poor transmission signal which is resulted from the extra attenuation of utilizing the high frequencies as well as their characteristics.

It merits saying, increasing the power transmission by +10 dBm slightly enhance the average rate by approximately extra (5-7%) of the UEs experience data rate more than 1Gbps. Other key finding can be deduced that the mobile location in terms of the mmWave base station plays an essential part of determining the data rate. Particularly, when the mobile station (MS) served by the (73 GHz) mmWave base station implies that the mobile (MS) will experience higher transmission rate than the mobile station (MS) which is served by the 38GHz as well as 28 GHz mmWave base station due to higher availability of the spectrum bandwidth taking into consideration how close the mobile station from the base station which operate at (73 GHz). More specifically, another point can be drawn from the curves depicted in the graphs above that adopting our proposed (AMSMC-S) scheme can significantly rise up the average rate of the overall mmWave system. Furthermore, the average rate distribution per user for the two aforementioned cell ranges (100m-150m) with different power constraints (30dBm-20dBm) utilizing of the proposed scheme can be briefly clarified:

a. Approximately as an average 45–50% of the UEs experience better average rate (> 1Gbps).
b. (55–50%) of the UEs experience average rate within the range from (200 Mbps–1Gbps).

Based on this, our new conceptual mmWave (mBSs) deployment with the novel link-adaptive scheme (AMSMC-S) outperforms the proposed approaches in the preliminary studies such as in [7], [13], [34], [35]. Thus, accelerating our pace to meet the required data rate for 5G cellular communication.

5. CONCLUSION

This paper proposes a novel Adaptive Multi-state mmWave Cell Selection (AMSMC-S) Scheme providing a new conceptual of mmWave (mBSs) deployment for outdoor users and outdoor infrastructure adopting flexible wireless communication with high transmission data rate. Particularly, when the (UEs) are closer to the mmWave base stations. An optimal cell selection has been considered based on maximum SINR value that are offered by three classes of mmWave base stations operating at three mmWave frequencies (73, 38 and 28 GHz). Multiple performance metrics are taken into consideration to obtain a detailed understanding of the potential issues and challenges, in addition to some encouraging results that pave the road for the near future cellular communications (5G).

The simulation results have proven that there is a direct correlation between the mmWave base stations density and the signal to interference plus noise ratio (SINR) value. On other hand, there is a tradeoff between the average rate and the frequency, which has been utilized by the serving base station. Moreover, approximately 45–55% of the UEs/Terminals experience better data rate (more than 1Gbps) with zero outage probability which opens the way for conducting more studies utilizing a flexible mechanism maintaining cross layer approach and guaranteeing efficient data delivering with user-centric quality along with different initial access mechanisms based on hybrid slicing and sharing the resources among different operators with/without taking the load balancing into consideration which remain as future work.

ACKNOWLEDGEMENTS

The authors gratefully acknowledge UTeM Zamalah Scheme, Universiti Teknikal Malaysia Melaka (UTeM).

REFERENCES

[1] Cisco, " Cisco Visual Networking Index: Forecast and Methodology, 2015-2020," *Forecast Methodol.*, p. 22, 2015. available [online] https://www.cisco.com/c/en/us/solutions/collateral/service-provider/visual-networking-index-vni/complete-white-paper-c11-481360.pdf.
[2] Cisco,"The Zettabyte Era: Trends and Analysis,". *Cisco 2017*, pp.1–29, 2017. available[online]http://www.netmode.ntua.gr/courses/postgraduate/video_communications/2014/VNI_Hyperconnectivity_WP.pdf.
[3] Jofri MH, Fudzee MF, Ismail MN, Kasim S, Abawajy J.Quality of experience (QOE) aware video attributes determination for mobile streaming using hybrid profiling. *Indonesian Journal of Electrical Engineering and Computer Science (IJEECS)*,2017; 8(3): 597–609.
[4] Lucrezia F, Marchetto G, Risso F, Santuari M, Gerola M. A Proposal for End-to-End QoS Provisioning in Software-Defined Networks. *International Journal of Electrical and Computer Engineering (IJECE)*, 2017;7(4): 2261–2277.
[5] Rappaport TS, Heath RW, Daniels RC, Murdock JN. Millimeter Wave Wireless Communications. United States: Pearson Education, 2014:14–15.
[6] Ford R, Zhang M, Mezzavilla M, Dutta S, Rangan S, Zorzi M. Achieving Ultra-Low Latency in 5G Millimeter

Wave Cellular Networks. *IEEE Communications Magazine*, 2017; 55(3):196–203.
[7] Rebato M, Boccardi F, Mezzavilla M, Rangan S, Zorzi M. Hybrid Spectrum Sharing in mmWave Cellular Netwroks. *IEEE Transactions On Cognitive Communications And Networking*, 2017; 3(2):155–168.
[8] Pi Z, Khan F. An introduction to millimeter-wave mobile broadband systems. *IEEE Communications Magazine*,2011; 49(6):101–107.
[9] Fund F, Shahsavar S, Panwar SS, Erkip E, Rangan S. *Resource sharing among mmWave cellular service providers in a vertically differentiated duopoly*. IEEE ICC 2017 Next Generation Networking and Internet Symposi. Paris, France. 2017:1–7.
[10] Rois JG, Lorenzo B, Gonźalez FJ, Burguillo JC. *Hetrogeneous Millimeter-wave/Micro-wave Architecture for 5G Wireless Access and Backhauling*. 2016 IEEE European Conference on Networks and Communications (EuCNC). Athens, Greece. 2016:179–184.
[11] Polese M, Giordani M, Mezzavilla M, Rangan S, Zorzi M. Improved Handover Through Dual Connectivity in 5G mmWave Mobile Networks. *IEEE Journal on Selected Areas in Communications*, 2017;35(9):2069–2084.
[12] Turgut E,Gursoy MC. Coverage in heterogeneous downlink millimeter wave cellular networks. *IEEE Transactions On Communications*,2017; 65(10): 4463–4477.
[13] Ford F,Cuba FG, Mezzavilla M, Rangan S. *Dynamic time-domain duplexing for self-backhauled millimeter wave cellular networks*. IEEE ICC 2015-Workshop on Next Generation Backhaul/Fronthaul Networks (BackNets 2015). London, United Kingdom.2015:13–18.
[14] Rappaport TS, MacCartney GR, Samimi MK, Sun S. Wideband Millimeter-Wave Propagation Measurements and Channel Models for Future Wireless Communication System Design. *IEEE Transactions on Communications*, 2015; 63(9):3029–3056.
[15] Salh A, Audah L, Mohd Shah NS, Hamzah SA. Adaptive Antenna Selection and Power Allocation in Downlink Massive MIMO Systems. *International Journal of Electrical and Computer Engineering (IJECE)*,2017; 7(6): 3521–3528.
[16] Ahmad SA, Datla D. Distributed Power Allocations in Heterogeneous Networks With Dual Connectivity Using Backhaul State Information. *IEEE Transactions on Wireless Communications*, 2015; 14(8):4574–4581.
[17] Astely D, Dahlman E, Fodor G, Parkvall S, Sachs J. LTE Release 12 and Beyond. *IEEE Communications Magazine*, 2013; 51(7):104–111.
[18] Sesia S, Baker M, Toufik I. LTE-the UMTS long term evolution: from theory to practice. UK:John Wiley & Sons, 25 Jan 2011.
[19] Soret B, Wang H, Pedersen KI, Rosa C. Multicell cooperation for LTE-advanced heterogeneous network scenarios," *IEEE Journals & Magazine*,2013;20(1):27–34.
[20] Ghosh A, Thomas TA, Cudak MC, Ratasuk R, Moorut P, Vook FW, Rappaport TS, MacCartney GR, Sun S, Nie S. Millimeter-wave enhanced local area systems: A high-data-rate approach for future wireless networks," *IEEE Journal on Selected Areas in Communications*, 2014;32 (6);1152–1163.
[21] Banani SA, Eckford AW, Adve RS. Analyzing Dependent Placements of Small Cells in a Two-Layer Heterogeneous Network with a Rate Coverage Constraint. *IEEE Transactions on VehicularTechnology*, 2016;65(12):9801–9816.
[22] Feng W, Wang Y, Lin D, Ge N, Lu J, Li S., When mmWave Communications Meet Network Densification: A Scalable Interference Coordination Perspective. *IEEE Journal on Selected Areas in Communications*, 2017; 35(7):1459–1471.
[23] Li Y, Pateromichelakis E, Vucic N, Luo J, Xu W, Caire G. Radio Resource Management Considerations for 5G Millimeter Wave Backhaul and Access Networks. *IEEE Communications Magazine*,2017; 55(6):86–92.
[24] Rappaport TS, Sun S, Mayzus R, Zhao H, Azar H, Wang K, Wong G, Schulz JK, Samimi M, Gutierrez F. Millimeter wave Mobile Communications for 5G Cellular: It Will Work!. *IEEE Access*, 2013;1:335–349.
[25] Ben-Dor E, Rappaport TS, Qiao Y, Lauffenburger SJ. *Millimeter-Wave 60 GHz Outdoor And Vehicle AOA Propagation Measurements Using A Broadband Channel Sounder*. 2011 IEEE Global Telecommunications Conference-GLOBECOM 2011. Kathmandu, Nepal. 2011:8–13.
[26] Rappaport TS, Ben-Dor E, Murdock JN, Qiao Y. *38 GHz And 60 GHz Angle-Dependent Propagation for Cellular & Peer-To-Peer Wireless Communications*. 2012 IEEE International Conference on Communications (ICC). Ottawa, ON, Canada. 2012: 4568–4573.
[27] Samimi M, Wang K, Azar Y, Wong JN, Mayzus R, Zhao H, Schulz JK, Sun S, Gutierrez F, Rappaport TS. *28 GHz angle of arrival and angle of departure analysis for outdoor cellular communications using steerable-beam antennas in New York City*. 2013 IEEE 77th Vehicular Technology Conference (VTC Spring). Dresden, Germany. 2013:1–6.
[28] Maccartney GR, Rappaport TS. *73 GHz Millimeter Wave Propagation Measurements for Outdoor Urban Mobile And Backhaul Communications in New York City*. 2014 IEEE International Conference on Communications (ICC). Sydney, NSW, Australia. 2014: 4862–4867.
[29] Piersanti S, Annoni LA, Cassioli D. *Millimeter Waves Channel Measurements And Path Loss Models*. 2012 IEEE International Conference on Communications (ICC). Ottawa,Canada. 2012: 4552–4556.
[30] Zhang H, Venkateswaran S, Madhow U. *Channel Modeling And MIMO Capacity for Outdoor Millimeter Wave Links*. 2010 IEEE Wireless Communication and Networking Conference. Sydney, NSW, Australia. 2010:8–13.
[31] Rappaport TS, Gutierrez F, Ben-Dor E, Murdock JN, Qiao Y, Tamir JI. Broadband Millimeter-Wave Propagation Measurements And Models Using Adaptive-Beam Antennas for Outdoor Urban Cellular Communications. *IEEE Transactions on Antennas and Propagation*, 2013; 61(4):1850–1859.
[32] Azar Y, Azar Y, Wong GN, Wang K, Mayzus R, Schulz JK, Hang Zhao H, Gutierrez F, Hwang D, Rappaport TS.

28 GHz propagation measurements for outdoor cellular communications using steerable beam antennas in New York city. 2013 IEEE International Conference on Communications (ICC). Budapest, Hungary. 2013:5143–5147.
[33] Murdock JN, Ben-Dor E, Qiao Y, Tamir JI, Rappaport TS. *A 38 GHz Cellular Outage Study For An Urban Outdoor Campus Environment*. 2012 IEEE Wireless Communications and Networking Conference (WCNC). Shanghai, China. 2012: 3085–3090.
[34] Akdeniz MR, Liu Y, Rangan S, Erkip E. *Millimeter wave picocellular system evaluation for urban deployments*. 2013 IEEE Globecom Workshops (GC Wkshps). Atlanta, GA, USA. 2013:105–110.
[35] Akdeniz MR, Liu Y, Samimi MK, Sun S, Rangan S, Rappaport TS, Erkip E. Millimeter Wave Channel Modeling and Cellular Capacity Evaluation. *IEEE Journal on Selected Areas in Communications*, 2014; 32(6):1164–1179.
[36] Singh S, Kulkarni MN, Andrews JG. *A tractable model for rate in noise limited mmWave cellular networks*. 2014 48th Asilomar Conference on Signals, Systems and Computers. Pacific Grove, CA, USA. 2015:1911–1915.
[37] Singh S, Zhang X, Andrews JG. Joint Rate and SINR Coverage Analysis for Decoupled Uplink-Downlink Biased Cell Associations in HetNets. *IEEE Transactions on Wireless Communications*, 2015;14(10):5360–5373.
[38] Bai T, Heath RW. *Analysis of Self-Body Blocking Effects in Millimeter Wave Cellular Network*. 2014 48th Asilomar Conference on Signals, Systems and Computers. Pacific Grove, CA, USA. 2014:1921–1925.
[39] Bai T, Heath RW. Coverage and Rate Analysis for Millimeter Wave Cellular Networks. *IEEE Transactions on Wireless Communications*, 2015;14(2):1100–1114.
[40] Giordani M, Mezzavilla M, Rangan S, Zorzi M. *Multi-connectivity in 5G mmWave cellular networks*. 2016 Mediterranean Ad Hoc Networking Workshop (Med-Hoc-Net). Vilanova i la Geltru, Spain. 2016:1–7.
[41] Deng J, Tirkkonen O, Hollanti RF, Chen T, Nikaein N. Resource Allocation and Interference Management for Opportunistic Relaying in Integrated mmWave/sub-6 GHz 5G Networks," *IEEE Communications Magazine*,2017;55(6):94–101.
[42] Attiah ML, Ismail M, Nordin R, Abdullah NF. *Dynamic multi-state ultra-wideband mm-wave frequency selection for 5G communication*. 2015 IEEE 12th Malaysia International Conference on Communications (MICC). Kuching, Malaysia. 2015:219–224.
[43] Hu F. Opportunities in 5G networks: A research and development perspective. United State : CRC press,30 Mar 2016.
[44] Rappaport TS, Murdock JN, Gutierrez F. State of the art in 60-GHz integrated circuits and systems for wireless communications. *Proceedings of the IEEE*, 2011; 99(8):1390–1436.
[45] Naga Bhushan, Li J, Malladi D, Gilmore R, Brenner D, Damnjanovic A, Sukhavasi RT, Patel C, Geirhofer S. Network Densification: The Dominant Theme for Wireless Evolution into 5G. *IEEE Communications Magazine*,2014; 52(2): 82–89.